Available online at www.sciencedirect.com
ScienceDirect
Thin Solid Films 515 (2006) 212 – 219
www.elsevier.com/locate/tsf

Assembling of redox proteins on Au(111) surfaces: A scanning probe microscopy investigation for application in bio-nanodevices

L. Andolfi, A.R. Bizzarri, S. Cannistraro *

Biophysics and Nanoscience Centre, INFM-CNISM, Dipartimento di Scienze Ambientali, Università della Tuscia, Viterbo, I-01100, Italy

Available online 19 January 2006

Abstract

The morphology and conductive properties of azurin molecules, chemically attached to sulfhydryl terminated alkanethiol monolayer assembled on Au(111) surface, are mapped at single molecule level and compared with those observed for the same molecule immobilised on bare Au(111). High-resolution Tapping Mode Atomic Force Microscopy shows that the protein molecules immobilised on modified gold, better reproduces the crystallographic height of the protein, than that immobilised on bare gold. Such a height recovering is also found in the Scanning Tunnelling Microscopy images. Consistently, a good tunnelling conduction of azurins on the modified gold electrode is demonstrated by Tunnelling Spectroscopy. Cyclic voltammetry measurements show, in addition, that the redox activity of azurin molecules covalently immobilised on sulfhydryl functionalised Au(111) surface is retained. These results are discussed in connection with possible use of this linker in the assembling of nano-hybrid systems.

Keywords: Scanning tunnelling microscopy; Atomic force microscopy; Azurin; Conduction; Sulfhydryl-terminated Au(111)

1. Introduction

The structural organization and the electron transfer (ET) properties of redox metalloproteins assembled on metallic surfaces are of central interest in the new area of nano-biotechnology. This field aims at creating devices of enhanced sensitivity that could be useful in biomedical and environmental research and drug discovery [1–3]. ET proteins offer a number of advantages in the construction of nano-biosensors due to their nanosized structure and their redox activity, which can be suitably tuned and electrochemically monitored [4,5]. The integration of ET proteins with a metallic electrode, with the possibility of establishing a good electrical contact among them, is a crucial issue in nano-biosensing. The ability of revealing an electrical signal, and therefore the sensitivity and reliability of these nano-biosensors, is strongly dependent on how protein immobilisation on the metal surface is achieved [6]. Obviously, it is also very important for the assembling of the ET proteins to ensure a preserved protein structure and function. An efficient electrical communication can be achieved by covalently linking the protein directly to the metal electrode. For such a purpose, thiols and/or disulfide groups present (or introduced by site-directed mutagenesis) in the protein molecules can be exploited, due to their ability to form stable bonds with the gold electrodes [7–13]. Direct protein adsorption on metallic surface provides the advantage to keep distances between the redox centre and the electrode surface within the range at which significant ET rates can occur [14]. Morphological and functional properties of some redox proteins assembled on bare gold have been studied by voltammetry, ellipsometry, X-ray photoelectron spectroscopy and mapped to single molecule level by scanning probe microscopy [7–18]. These techniques have shown that the assembled redox proteins can retain, in some cases, their function upon immobilization on gold [7,9,11,15,16]. In other cases, a partial protein unfolding has been observed by height analysis in Atomic Force Microscopy (AFM), in conjunction with ellipsometry studies on protein monolayers [7,8,17,18]. It has been also observed that some redox proteins, directly attached to a metal, do not give any electrochemical signal [19–21]. These results could be related to the occurrence of an extensive protein interaction with the metallic surface, which can eventually lead to a loss of protein native conformation.

* Corresponding author. Tel.: +39 0761 357136; fax: +39 0761 357179.
E-mail address: cannistr@unitus.it (S. Cannistraro).

0040-6090/$ - see front matter © 2005 Elsevier B.V. All rights reserved.
doi:10.1016/j.tsf.2005.12.115

However, Scanning Tunnelling Microscopy (STM) operating in constant current mode almost always underestimates the physical height of the assembled proteins on Au(111) surface with respect to other techniques (crystallography, AFM and ellipsometry) [11,13,15,16,22–25].

A more gentle linking of the proteins to metallic electrodes can be attained by chemically modifying the metal surface by assembling a monolayer of short alkane molecules, on the top of which the proteins can be anchored [26–29]. A variety of small organic molecules can be used to create sulfhydryl-terminated alkanethiol monolayer on a gold surface, which can react with thiol groups of the biomolecules leading to a well defined protein immobilization [30,31]. It should be taken into account that a suitable linker should not significantly affect the ET rate due to its length.

In this work, we used an amine-termined monolayer formed by self-assembling cysteamine molecules on Au(111), which was reacted then with the heterobifunctional linker *N*-succinimidyl-*S*-acetylthiopropionate to obtain a sulfhydryl surface [32,33]. On this sulfhydryl functionalised Au(111) surfaces we tethered azurin (AZ) molecules. AZ is a small redox copper protein, which bears an exposed disulfide group, located in a region opposite to the redox site and suitable for a covalent anchoring on both bare and thiol-terminated gold surface. As schematically shown in Fig. 1A, AZ molecules assembled on the modified Au(111) are expected to exhibit a molecular orientation similar to that obtained on bare gold (see Fig. 1B), but with the protein residues sheltered from a direct strong interaction with gold [34].

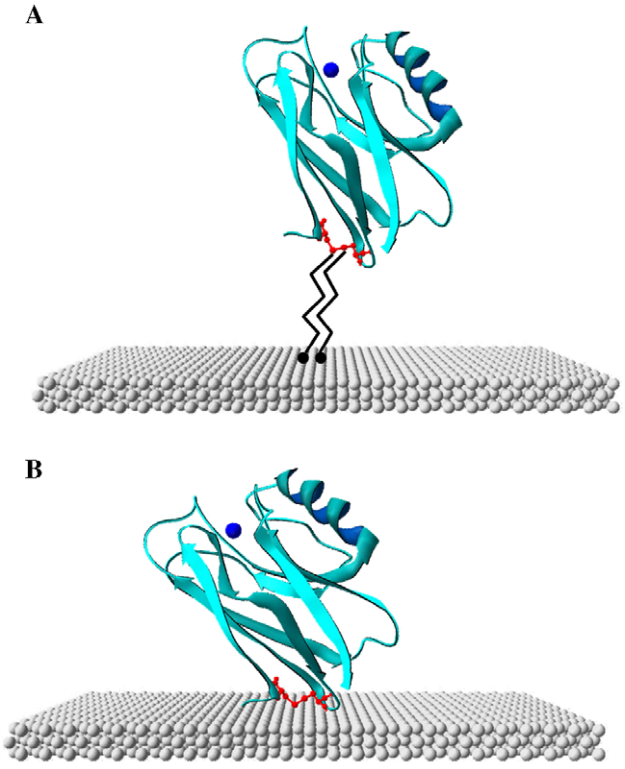

Fig. 1. Schematic view of AZ molecular orientation upon reaction of S–S moiety with the sulfhydryl terminated Au(111) surface (A); AZ molecular orientation on bare Au(111) when protein is anchored via S–S group (B).

The morphological and conductive properties of individual AZ proteins assembled on sulfhydryl-terminated monolayer have been investigated by high-resolution Tapping Mode AFM (TMAFM), STM and Scanning Tunnelling Spectroscopy (STS), and compared with those obtained for AZ on bare Au(111). The vertical size of AZ molecules immobilised on thiol-modified Au(111), evaluated by TMAFM, closely matches the crystallographic value [35], while on bare gold a reduced AZ height has been generally obtained. STM images of AZ molecules on thiol functionalised Au(111) show single-molecule structures with a height notably enhanced as compared to that obtained for AZ, and in general for other biomolecules, adsorbed on gold. Moreover, STS data reveal a good tunnelling conduction for AZ immobilised on sulfhydryl terminated gold.

Analogously to what was found for the AZ proteins anchored directly on gold, the redox activity of AZ molecules on chemically modified gold surface is retained, as demonstrated by cyclic voltammetry (CV) measurements.

2. Experimental

AZ, cysteamine and *N*-succinimidyl-*S*-acetylthiopropionate (SATP) have been purchased from Sigma Chemical Co., and used without further purification. Gold substrates (Arrandee) consist of a vacuum evaporated thin gold film (thickness 200 nm) on borosilicate glass. They have been annealed with a butane flame to obtain re-crystallized Au(111) terraces. The quality of the annealed gold surface was assessed by STM, which showed atomically flat (111) terraces over hundreds of nanometers.

The molecules were adsorbed on Au(111) surface by directly incubating the annealed substrates with AZ protein solution (3.5 μM in 50 mM NH_4Ac pH 4.8) at 4 °C for times ranging between 30 min and few hours.

The Au(111) surface functionalization was made by immersing freshly annealed substrates into a 1 mM ethanolic solution of cysteamine for 24 h. SATP (20 mM, 10% DMSO and 90% PBS pH 7.0) was reacted with the cysteamine monolayer for 2 h. The protecting group of the sulfhydryl was removed by exposing the monolayer to a solution of 0.5 M of hydroxylamine in 50 mM PBS pH 7, 25 mM EDTA, and 50 mM DTT for 20 min. The sulfhydryl surface was then reacted with AZ solution (20 μM in 50 mM NH_4Ac pH 4.8) for 1 h at room temperature. Samples were then rinsed with ultrapure water and blown dry with pure nitrogen.

TMAFM measurements were performed with a Nanoscope IIIa/Multimode, Digital Instruments equipped with a 12-μm scanner operating in tapping mode in ultra-pure water (18.2MΩ cm). Silicon probes (Digital Instruments), 100 or 200 μm long, with nominal radius of curvature less than about 20 nm and spring constants of 0.15 and 0.57 N/m, respectively, were used. Resonance peaks in the frequency response of the cantilever were chosen in the range of 8–30 kHz. Free oscillation of the cantilever was set to have root-mean-square amplitude corresponding to 10 nm. In each measurement, the set point was adjusted before scanning, to

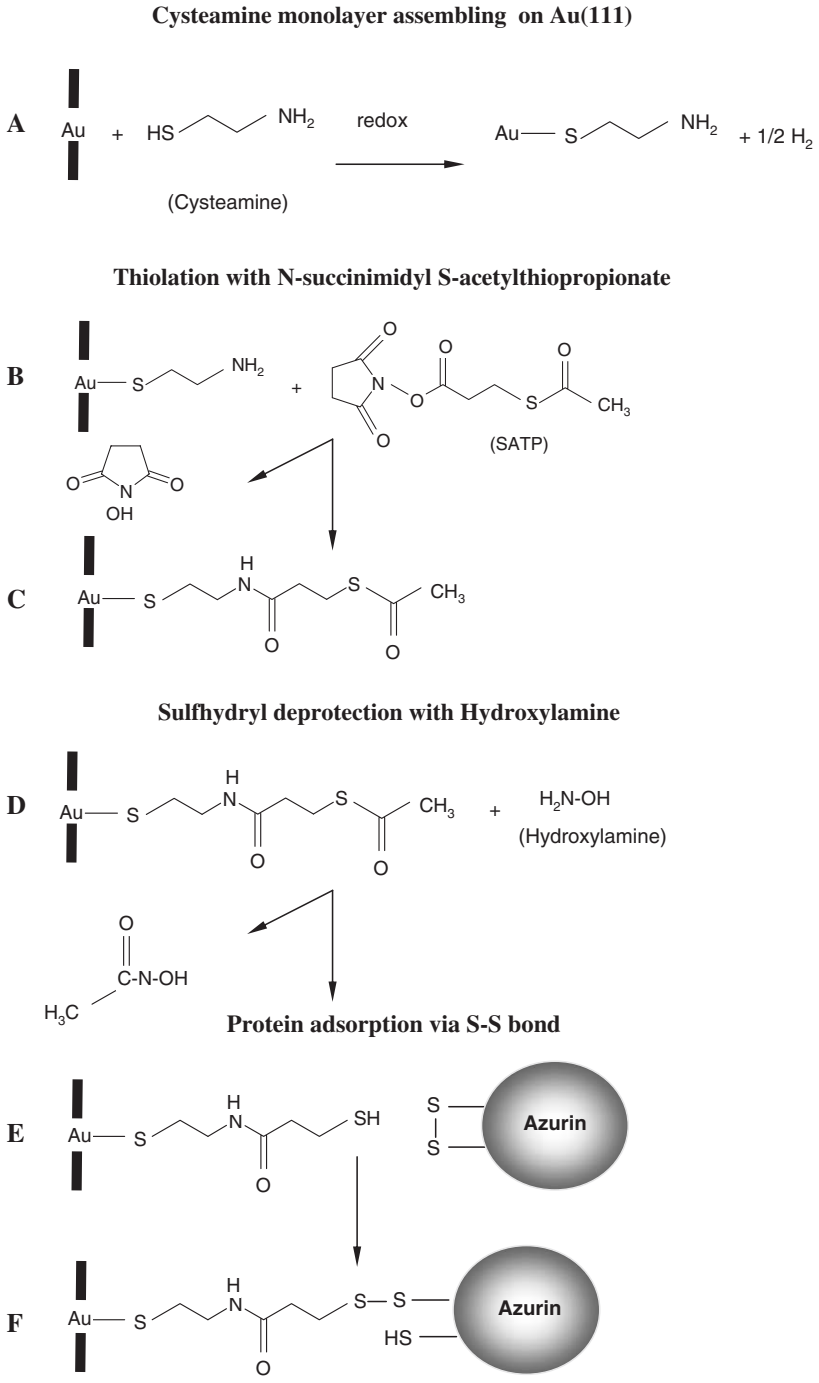

Fig. 2. Surface reaction scheme illustrating the steps involved in formation of chemically modified Au(111) surface. (A) self-assembling of cysteamine on gold via SH group; (B–C) reaction of the heterobifunctional linker SATP with the cysteamine monolayer forming an amide bond; (D) deprotection of the sulfhydryl by removing the acetyl protecting group; (E–F) the sulfhydryl active group reaction with the S–S group of AZ.

minimise the force between the tip and the sample. The height related to the z-piezo and the curvature radius of the tips were calibrated by using 5 nm gold colloids deposited on a glass slide coated with (3 mercaptopropyl)-trimethoxysilane [36].

A Picoscan system (Molecular Imaging) equipped with a 10 μm scanner with a final preamplifier sensitivity of 1 nA/V was used for STM and STS measurements. STM tips were prepared by mechanically cutting Pt/Ir wires (Goodfellow). For STS experiments, Current–voltage ($I-V$) curves were obtained by setting the gap between the STM tip and the protein at a tunnelling current of 50 pA and bias of −1 V. Then the feedback was disengaged and the current was monitored as the substrate potential is swept over ±1 V. Every single sweep was collected in 0.01 s.

Cyclic voltammetry was performed with a PicoSTAT bipotentiostat (Molecular Imaging Co.). The electrochemical cell housed two Pt wires as counter and pseudo-reference electrodes and was filled with 150 μl of 50 mM NH_4Ac pH 4.8. The potential of Pt wire was calibrated against a standard

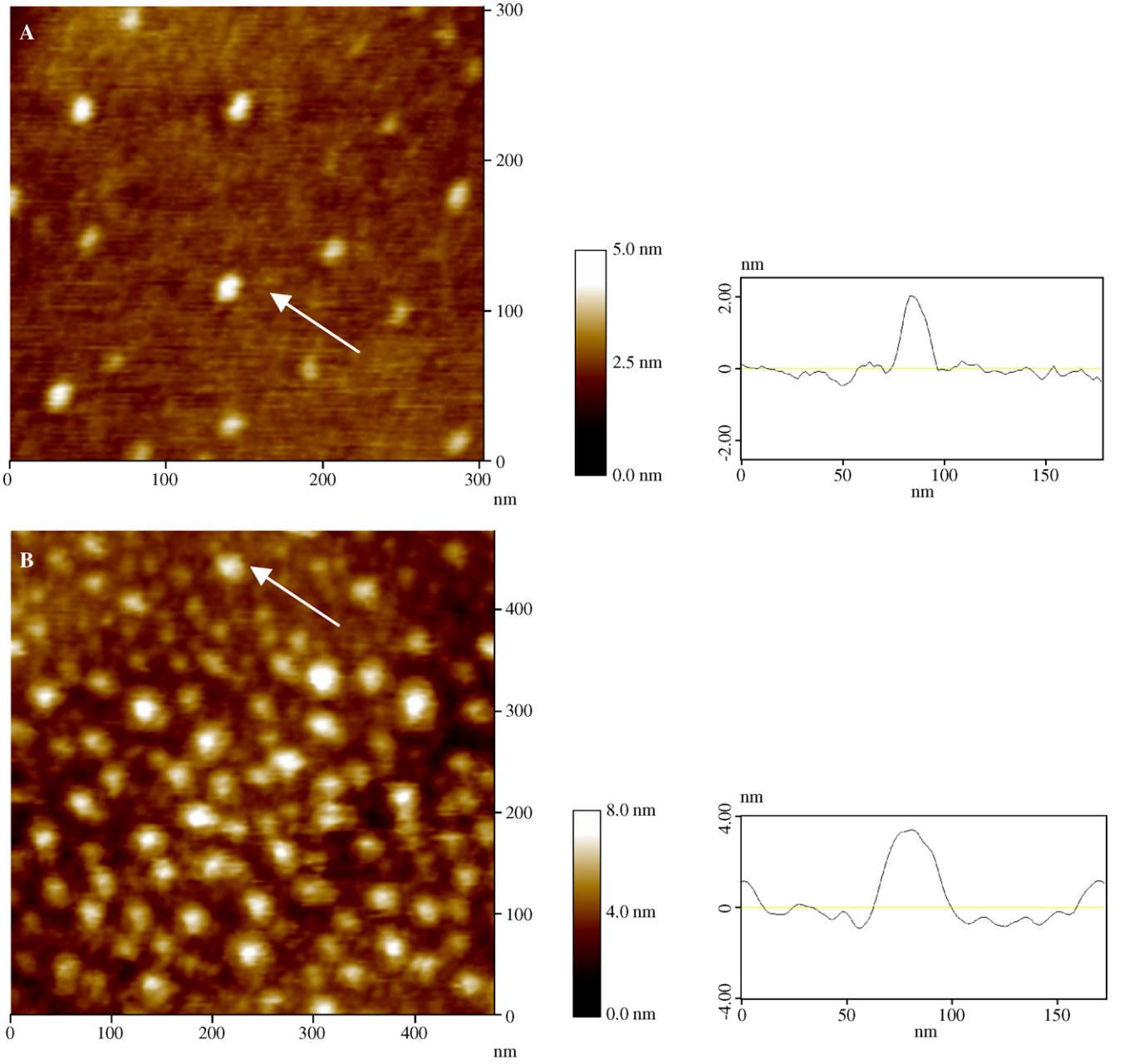

Fig. 3. Representative TMAFM images acquired on AZ molecules directly adsorbed on Au(111) surface (A), and on AZ adsorbed on cysteamine-SATP monolayer (B). Cross section profiles of the molecules indicated by the white arrows are reported in the lateral panels.

calomel electrode (SCE). All potentials are then quoted relative to SCE.

3. Results and discussion

The thiol-functionalization of Au(111) surface, for oriented AZ immobilization, was formed according to the reaction scheme depicted in Fig. 2. The cysteamine molecules self-assemble on Au(111) via their thiol group generating an amine terminated monolayer (Fig. 2A). These groups can then react with the heterobifunctional linker SATP (Fig. 2B), which on one hand forms a stable amide linkage with the amine group, while on the other exposes an acetyl group protecting a sulfhydryl group (Fig. 2C). By treating the monolayer with hydroxylamine the acetyl group is removed revealing an active sulfhydryl surface (Fig. 2D). The sulfhydryl groups are then exposed to react with the disulfide bond of AZ (Fig. 2E,F). This attachment chemistry has been confirmed by spectroscopic studies [32,33], and produces an ordered uniform monolayer suitable for proteins tethering and for nanoscale studies.

The morphology of AZ molecules assembled on bare Au(111) and on the cysteamine-SATP monolayer assembled on gold was characterized by TMAFM. This technique, while on one hand gives minor information about the lateral molecular size owing to the broadening effects introduced by the tip size, on the other accurately estimates the vertical dimension of the biomolecules over the substrates. Fig. 3A

shows an AFM image of AZ molecules directly adsorbed on Au(111), via the S–S group as widely demonstrated [7,8,11,17]. In this image, single molecules are clearly detected on a quite smooth surface, which display a root-mean-square roughness (RMS) of 0.13±0.01 nm. The protein height with respect to the Au(111) substrate was evaluated by a cross section analysis on individual molecules (see cross section profile of Fig. 3A). Over a collection of 100 molecules, we obtained a gaussian distribution with a mean value of 1.7 nm and a standard deviation of 0.5 nm, consistent with previous studies [7,8,17]. This value appears to be lower than what was expected by the crystallographic structure, if the AZ assembling on gold, via S–S group, would occur in a standing up arrangement as illustrated in Fig. 1B [7]. Such finding could be likely associated with a strong AZ interaction with the noble metal, that might either force the protein to adopt a lying down configuration above the substrate or even to cause a partial protein denaturation.

A representative AFM image acquired on AZ molecules adsorbed on the cysteamine-SATP monolayer assembled on Au(111) is shown in Fig. 3B. Over a surface background with a roughness RMS=(0.40±0.04) nm, single AZ molecule are well resolved as homogeneous globular shape structures. The molecular vertical dimension of AZ on the monolayer is evaluated by cross section analysis on individual molecules (see height profile of Fig. 3B), also taking into account contributions of the background roughness. The obtained heights are plotted in the histogram of Fig. 4. The distribution is centred at a mean value of 3.4 nm with a standard deviation of 0.8 nm. This value, significantly higher than that observed for AZ directly immobilised on Au(111), well matches the vertical structure of the protein, as evaluated by crystallography [35]. Such result indicates that the interactions between the amino acid residues and the noble metal are screened upon the binding of AZ (via its S–S bridge) with the thiol group of the

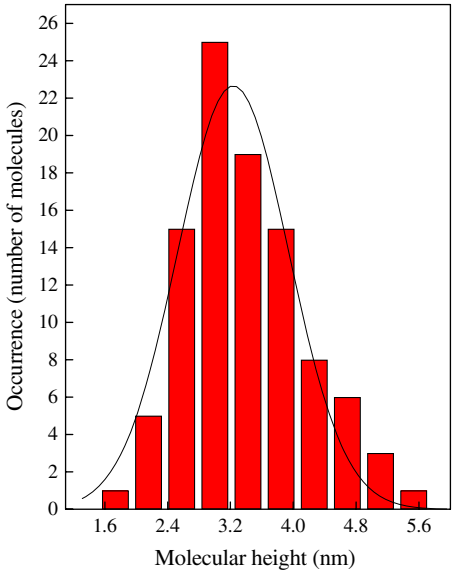

Fig. 4. Statistical analysis of AZ molecular height on chemically modified Au(111) surface, mean height value=3.4 nm and σ=0.8 nm. Data are obtained from individual cross section profiles over 100 molecules.

monolayer, and that under these conditions the protein may adopt a standing up configuration on the substrate, with a three-dimensional structure closer to its native form.

A further characterization of AZ molecules assembled on bare and cysteamine-SATP modified Au(111) was performed by STM, operating in constant current mode, where the molecular height is registered as a function of the measured current. The protein lateral dimension can be precisely evaluated by STM, where tip is known to induce a minor convolution with respect to AFM. Fig. 5A shows an STM image of single AZ molecules adsorbed on Au(111); they are stable upon repetitive scans and present a lateral size of 4.5±0.9 nm (see cross section profile of Fig. 5A), consistently with other works [7,8,11,17]. The molecular height, on the contrary, is found to be 0.5±0.1 nm, appearing significantly lower than the physical height evaluated by crystallographic studies [35]. This is, however, a general characteristic of STM images obtained on biomolecules self-assembled on conductive substrates [11,13,16,22–25], and it is very likely related to the low conductivity of biomolecules. Such an aspect has been deeply addressed in a previous work, where it is shown that the real vertical dimension is recovered by STM only when uniformly metallic nanoparticles deposited on Au(111) substrates are imaged [25]. For redox proteins adsorbed on gold, variations of the molecular height have been observed by performing STM under electrochemical control, which has indicated that, in some cases, tunnelling current flow through the redox protein can be properly modulated upon tuning the substrate potential with the respect to the redox potential of the protein [13,23].

Surprisingly, we find that the STM height of the AZ molecules assembled on the cysteamine-SATP monolayer is 1.8 nm with a standard deviation of 0.4 nm (see Fig. 5B). Such enhanced molecular height is put into evidence by a representative height profile shown in the lateral panel of Fig. 5B. The protein lateral size, obtained in the STM images, is 3.7 nm with a standard deviation of 0.8 nm, consistent with that found for AZ on bare gold. The vertical and lateral dimensions of the protein molecules appear to be reproducible after repetitive scans. The significant increment in the measured molecular height can result from a more efficient electron tunnelling between the tip and the substrate through the protein when covalent immobilization is achieved by the cysteamine-SATP linker.

To get additional information about the conduction of single AZ immobilised on cysteamine-SATP monolayer, $I–V$ curves were registered by STS. In these measurements the tip was positioned on top of a single protein, the feedback loop was temporarily disengaged and the tunnelling current was monitored as the sample bias was ramped in the range of ±1 V. Each single $I–V$ curve, acquired on a single protein, consists of the average over 10 consecutive bias sweeps. These measurements were repeated on several molecules and were averaged over 100 bias sweeps. The resulting curve for AZ assembled on cysteamine-SATP, compared with those of the bare and cysteamine-SATP modified Au(111), are shown in Fig. 6.

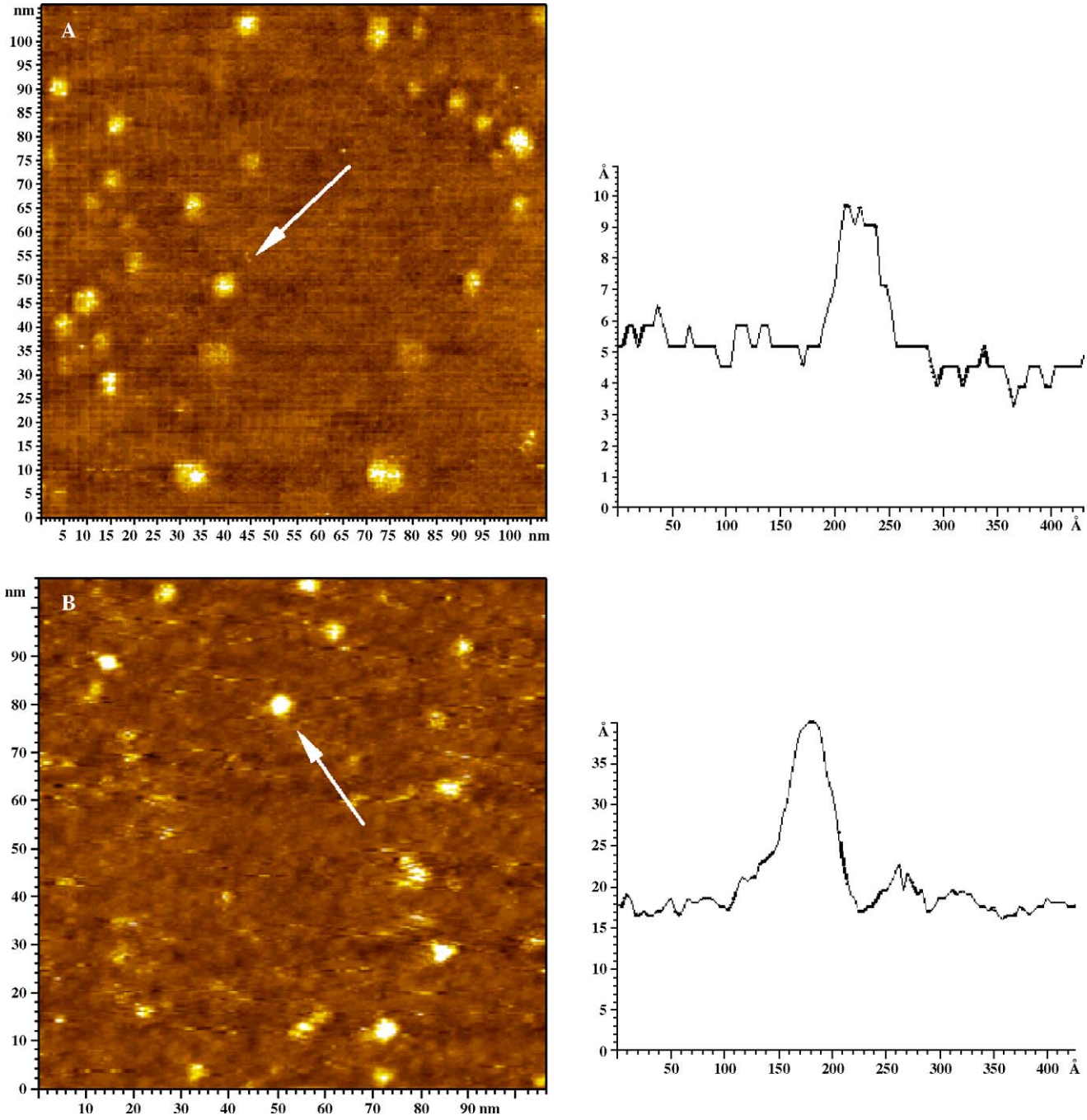

Fig. 5. Constant current STM images of AZ molecules immobilised on Au(111) (A) and of AZ anchored on cysteamine-SATP monolayer assembled on gold (B). The cross section profiles of the molecules (indicated by the white arrows) are shown in the lateral panels. Tunnelling current 50 pA and voltage bias −1 V; scan rate 3.0 Hz.

The three curves appear to be superimposed in the negative part of the $I-V$ spectrum, while at positive bias (about +0.9 V) we can observe that the monolayer deposited on gold registers a small reduction of the current response. However, for AZ bound on the monolayer the current response increases approaching that obtained for bare gold. A slight asymmetry for AZ assembled on the functionalised gold can be noticed, which, in any cases, is not as pronounced as that observed for AZ on bare Au(111) [7,17]. We remark that, although the STS spectra show that the AZ tethered on cysteamine-SATP monolayer are equally conductive within a range of +1 and −1 V, we found some difficulties when STM imaging of these sample was performed at positive biases (between +0.2 and +1 V). In this case, the imaging appears strongly disturbed and single molecule could not be detected. This behaviour is generally indicative of a strong interaction between the STM tip and the imaged sample. Conversely, such phenomenon is not observed for AZ molecules directly anchored on gold, which can be clearly imaged at positive and negative bias values, without considerable variations in molecular height. Although a good tunnelling conduction is revealed, the discrepancy between spectroscopy and imaging observed both

for AZ immobilised on bare and modified gold is presently not clear and requires further investigations.

Finally, the functionality of immobilised AZ on modified gold electrodes was investigated by CV in which the faradaic current was measured as function of the substrate potential. No redox response was observed for the SATP-cysteamine functionalised Au (111) substrate in 50 mM ammonium acetate pH 4.8. A current response was obtained after overnight incubation of the activated monolayer with AZ solution. The voltammogram of Fig. 7 shows a pair of peaks corresponding to the oxidation and reduction peak of the protein on the cysteamine-SATP monolayer. The voltammetric response is stable up to few hours of measurements. The formal redox potential ($E_{1/2}$), calculated as $E_{1/2}=(E_{pa}+E_{pc})/2$, is 280± 20 mV, which appears to be shifted to more positive values than that reported for AZ directly anchored on gold (165–175 mV) [15]. The linear dependence of the peak current on the scan rate is consistent with electroactive molecules being confined to the surface (see inset of Fig. 7). The separation between the anodic and the cathodic peaks ΔE_p, is 170 mV (at a scan rate of 100 mV/s) and it is dependent on the scan rate showing a quasi-reversible kinetics. Moreover, the ΔE_p value obtained on the modified gold is greater than that of AZ adsorbed on bare Au(111), indicating a slower electron transfer process. The shift of the midpoint redox potential and the indication of a slower ET are very likely the result of the cysteamine-SATP monolayer, being interposed between the protein and the Au(111) surface. An estimate of the surface coverage with electroactive AZ molecules can be obtained from Eq. (1)

$$I_p(v) = \left(Nn^2F^2/4RT\right)_v \quad (1)$$

where I_p is the peak current (anodic or cathodic), v is the voltage scan rate, N is the number of redox-active sites on the surface, n is the number of electrons transferred, F the Faraday constant, R the gas constant and T the temperature. From the slope of I_p versus scan rate with $n=1$, we estimate a surface coverage of 2.1×10^{13} molecules cm^{-2}. This value, in good agreement with the expected coverage for a molecule with a lateral dimension of about 4 nm [15], confirms a high degree of structural retention of the AZ proteins on the modified gold.

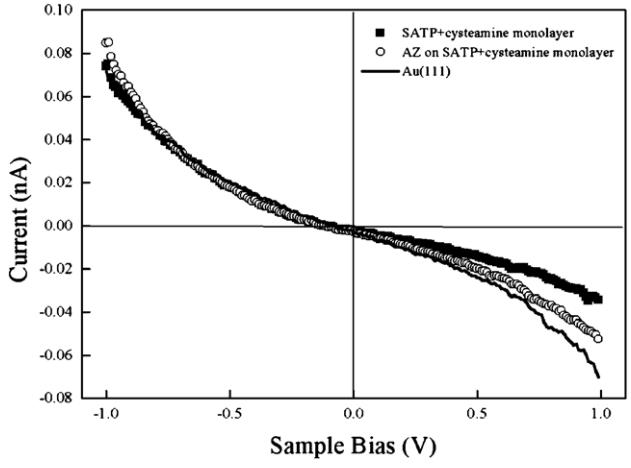

Fig. 6. $I-V$ curves recorded in ambient conditions on AZ molecules (open circle), cysteamine-SATP monolayer (square) and Au(111) (solid line). The engage tunnelling current and voltage bias are 50 pA and −1 V, respectively.

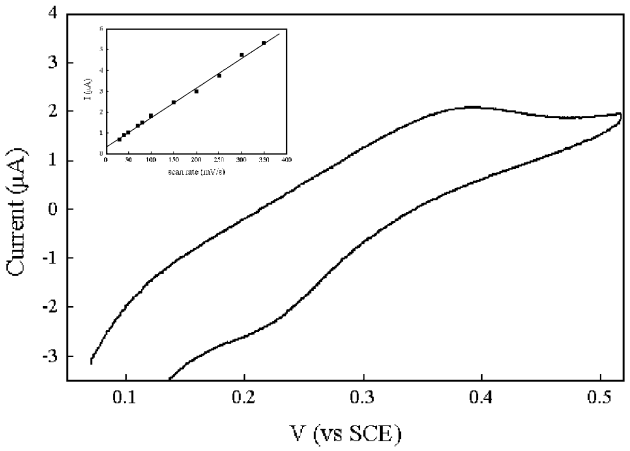

Fig. 7. Voltammogram of AZ immobilised on SATP-cysteamine monolayer recorded at a scan rate of 100 mV/s in 50 mM NH_4Ac pH 4.8. The inset shows the change in oxidation current with increasing scan rate.

4. Conclusions

The present study indicates that AZ molecules can be firmly and functionally assembled on both bare and suitably modified Au(111) surfaces. The comparison of the two immobilization strategies shows that the cysteamine-SATP monolayer interposed between the gold surface and the AZ molecules, aids to reduce the protein–metal interactions, resulting in a standing up configuration of AZ molecules over the substrate with protein structure closer to its native form. Strikingly, we found that the sulfhydryl terminated alkanethiol monolayer is able to facilitate the tunnelling current through the protein. Hence, the cysteamine-SATP linker appears to be an effective way for integrating the redox metalloproteins with a gold electrode, and this represents an important result, especially in view of a nano-biotechnology application of these proteins.

Acknowledgments

This work has been partially supported by the FIRB-MIUR Project “Molecular Nanodevices” and a PRIN-MIUR 2004 project. L. Andolfi acknowledges the Research Grant MIUR “Rientro dei Cervelli”.

References

[1] R. Freitas, Nanomedicine: Nanotechnology, Biology and Medicine, vol. 1, 2005, p. 2.
[2] H. Klefenz, Eng. Life Sci. 4 (2004) 211.
[3] C.R. Lowe, Curr. Opin. Struck. Biol. 10 (2000) 428.
[4] I. Willner, B. Willner, Trends Biotech. 19 (2001) 222.
[5] G. Gilardi, A. Fantuzzi, Trends Biotech. 19 (2001) 468.
[6] E. Katz, V. Heleg-Shabtai, B. Willner, I. Willner, A.F. Bückmann, Bioelectrochem. Bioenerg. 42 (1997) 95.
[7] B. Bonanni, D. Alliata, L. Andolfi, A.R. Bizzarri, S. Cannistraro, in: C.P. Norris (Ed.), Surface Science Research Developments, Nova Science Publishers, Inc., 2004.
[8] J.J. Davis, H.A.O. Hill, Chem. Commun. (2002) 393 .

[9] H.A. Heering, F.G.M. Wiertz, C. Dekker, S. de Vries, J. Am. Chem. Soc. 126 (2004) 11103.
[10] L. Andolfi, S. Cannistraro, G.W. Canters, P. Facci, A.G. Ficca, I.M.C. Van Amsterdam, M.Ph. Verbeet, Arch. Biochem. Biophys. 399 (2002) 81.
[11] Q. Chi, J. Zhang, J.U. Nielsen, E.P. Friis, I. Chorkendorff, G.W. Canters, J.E.T. Andersen, J. Ulstrup, J. Am. Chem. Soc. 122 (2000) 4047.
[12] J. Hang, Q. Chi, T. Albrecht, A.M. Kuznestov, M. Grubb, A.G. Hansen, H. Wackerbarth, A.C. Welinder, J. Ulstrup, Electrochim. Acta 50 (2005) 3143.
[13] L. Andolfi, B. Bonanni, G.W. Canters, M.Ph. Verbeet, S. Cannistraro, Surf. Sci. 530 (2003) 181.
[14] R.A. Marcus, N. Sutin, Biochim. Biophys. Acta 811 (1985) 265.
[15] L. Andolfi, D. Bruce, S. Cannistraro, G.W. Canters, J.J. Davis, H.A.O. Hill, J. Crozier, M.Ph. Verbeet, C.L. Wrathmell, Y. Astier, J. Electroanal. Chem. 565 (2004) 21;
J.J. Davis, D. Bruce, G.W. Canters, J. Crozier, H.A.O. Hill, Chem. Commun. (2003) 576.
[16] B. Bonanni, D. Alliata, A.R. Bizzarri, S. Cannistraro, Chem. Phys. Chem. 4 (2003) 1183.
[17] A.R. Bizzarri, L. Andolfi, M. Stchakovsky, S. Cannistraro, J. Nanotechnol. 1 (2005) 100.
[18] B. Schnyder, R. Koetz, D. Alliata, P. Facci, Surf. Int. Anal. 34 (2002) 40.
[19] D.E. Reed, F.M. Hawkridge, Anal. Chem. 59 (1987) 2334.
[20] F.A. Armstrong, Struct. Bond. 72 (1990) 137.
[21] Y. Zhou, T. Nagaoka, G. Zhu, Biophys. Chem. 79 (1999) 55.
[22] J.J. Davis, D.A. Morgan, C.L. Wrathmell, A. Zhao, IEE Proc.-Nanobiotechnol. 151 (2004) 37.
[23] P. Facci, D. Alliata, S. Cannistraro, Ultramicroscopy 89 (2001) 291.
[24] D. Losic, J.G. Shapter, J.J. Gooding, Langmuir 18 (2002) 5422.
[25] D. Alliata, L. Andolfi, S. Cannistraro, Ultramicroscopy 101 (2004) 231.
[26] Q. Chi, J. Zhang, J.E.T. Andersen, J. Ulstrup, J. Phys. Chem., B 105 (2001) 4669.
[27] M.J. Tarlov, E.F. Bowden, J. Am. Chem. Soc. 113 (1991) 1847.
[28] A.K. Gaigalas, G. Niaura, J. Colloid Interface Sci. 193 (1997) 60.
[29] O. Cavalleri, C. Natale, M.E. Stroppolo, A. Relini, E. Cosulich, S. Thea, M. Novi, A. Gliozzi, Phys. Chem. Chem. Phys. 2 (2000) 4630.
[30] J. Zhang, H.E.M. Christensen, B.L. Ooi, J. Ulstrup, Langmuir 20 (2004) 10200.
[31] J. Zhang, A.C. Welinder, A.G. Hansen, H.E.M. Christensen, J. Ulstrup, J. Phys. Chem., B 107 (2003) 12480.
[32] E.A. Smith, M.J. Wanat, Y. Cheng, S.V.P. Barreira, A.G. Frutos, R.M. Corn, Langmuir 17 (2001) 2502.
[33] G.J. Wegner, H.J. Lee, G. Marriott, R.M. Corn, Anal. Chem. 75 (2003) 4740.
[34] X. Chen, R. Ferrigno, J. Yang, G.M. Whiteside, Langmuir 18 (2002) 7009.
[35] H. Nar, A. Messerschmidt, R. Huber, M. van de Kamp, G.W. Canters, J. Mol. Biol. 218 (1991) 427.
[36] B. Bonanni, S. Cannistraro, J. Nanotechnol. 90106 (2005) 1.